Heliyon 10 (2024) e27179

Contents lists available at ScienceDirect

Heliyon

journal homepage: www.cell.com/heliyon

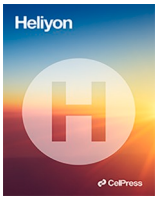

Research article

Design optimization of irregularity RC structure based on ANN-PSO

Xun Zhang

School of Management, Guangzhou University, Guang Zhou, 510006, GuangDong, China

ARTICLE INFO

Keywords:
Design optimization
Irregularity RC structure
ANN-PSO
Seismic performance

ABSTRACT

Seismic design principles advocate for simple and regular structures to minimize earthquake damage. However, this frequently does not lead to unique and aesthetically pleasing designs, leading some engineers to select irregular structures despite the potential risks. The primary aim of this investigation is to achieve the optimal design of torsional irregularity coefficients for planar irregular reinforced concrete (RC) frames under static and dynamic loads, utilizing a 3D 6-layer model. Structural ground vibration analysis was conducted using the ETABS software. By imposing limits on the torsional irregularity coefficients for each layer of the frame layout, we subsequently applied the combination of artificial neural networks (ANN) with the particle swarm optimization (PSO) algorithm, namely ANN-PSO, to address the size distribution issue across the structure. The design variables included the dimensions of the columns located in each layer of the layout. The results demonstrate that the ANN-PSO algorithm optimizes the cross-sectional area of columns with significant variations. The coefficients of the torsion inequality rule in the optimized solution closely approach the minimum values. The dimensions and orientations of the optimized columns slightly differ from the pre-optimized scheme. In the optimized scheme, the coefficients of the torsional irregularity in the Y-direction meet the requirements, preventing any torsional irregularities from occurring. The research presented an effective method, including an innovative combination of ANN-PSO and the finite element method (FEM), for designing RC structures. The findings of the research provided a practical solution to fulfill torsional regularity criteria, indicating the proposed approach is an effective method for the economical and safe design of RC structures in earthquake-prone areas. The outcomes of the present study highlighted the innovative framework to achieve optimal and safe designs for irregular RC structures while minimizing torsional damage during earthquakes.

1. Introduction

Reinforced concrete (RC) combines concrete with strong resistance to compression and steel with high resistance to tension. In the field of civil engineering, it is essential to gain comprehensive knowledge about the behaviors of materials in various conditions to employ for civil engineering projects [1–5]. Furthermore, it is important to have a comprehensive understanding of the different fracture and failure mechanisms that lead to the destruction of the strength of materials [6,7]. RC structures play a crucial role in contemporary construction due to several advantages, including durability, high strength, flexibility, fire resistance, and economic efficiency. Therefore, in order to enhance the efficiency of RC structures, many research studies have been conducted in recent years

E-mail address: zhx6377@163.com.

https://doi.org/10.1016/j.heliyon.2024.e27179
Received 18 September 2023; Received in revised form 25 February 2024; Accepted 26 February 2024
Available online 27 February 2024

[8–12].

Experimental research is a vital component in the design of concrete structures [13,14]. Laboratory studies allow the evaluation of concrete properties, material properties analysis, investigation of failure mechanisms, simulation of various environmental conditions like extreme temperatures and loading conditions, and development and assessment of different structural elements [15–19]. Despite the mentioned advantages of experimental works, they suffer from scale limitations and are costly and time-consuming [20]. Nowadays, significant advancements have been made in the field of structural design using numerical analysis and finite element methods (FEM) that enable engineers to accurately simulate the three-dimensional behavior of large-scale structures [21,22]. Moreover, in parallel with laboratory studies, computational intelligence methods have seen a significant increase in related structural engineering and have demonstrated practical tools for optimizing structural designs, improving material utilization, and accurately predicting possible failure points [23–27]. Many investigations have emphasized the significance of understanding and employing data-driven and evolutionary algorithms for the safe and economical design of structures.

The artificial neural network (ANN) has emerged as a popular and powerful method for solving engineering problems [28,29]. ANN resembles the neural architecture of the human brain by employing an enormous number of interconnected neurons that operate in parallel to analyze and interpret data [30]. ANN, as well as the good applicability of particle swarm optimization (PSO) algorithms for solving engineering structural optimization problems. ANN is often used as a proxy model for PSO fitness functions, i.e., ANN-PSO [31–33]. The combination of the ANN-PSO model indicated an efficient, practical, and simple approach for practical engineering applications regarding RC structures [34–36]. Bayari et al. [37] employed the ANN-PSO for the estimation and assessment of collapse danger and the determination of structural reliability. Nguyen et al. [38] have developed ANN-PSO to predict the shear strength of reinforced concrete (RC) beams. The mentioned studies illustrated that the hybridization of ANN with PSO improves convergence and enhances the accuracy of the quality of results for modeling concrete structure elements. The need to apply optimization-based evolutionary and meta-heuristic algorithms in RC structural design is highlighted by Afzal et al. [39]. Sánchez-Olivares and Tomás [40] presented the Firefly Algorithm (FA) and GA to determine the most cost-effective design of RC subjected to compression forces. Hong et al. [41] illustrated the effectiveness of ANN-based optimization methods in improving the design process of structural elements related to pre-tensioned concrete beams. Yazdani et al. [42] demonstrated that their gravitational search algorithm (GSA) could significantly benefit engineers in the design of reinforced concrete (RC) structures under seismic loading, taking into account nonlinear soil-structure interaction effects. Esfandiari et al. [43] proposed a novel approach combining multi-criterion decision-making (DM) and PSO techniques. Their approach was used to optimize RC structures under seismic loads. Martins et al. [44] developed an optimization-based computational approach for designing RC-framed structures, focusing on minimizing costs while meeting strength and serviceability requirements as defined by Eurocode 2. Mergos [45] conducted a study implementing a surrogate-based optimization (SBO) method for the economical design of RC frames, specifically examining a 4-story and a 12-story building as per Eurocode regulations.

The optimal design of irregular structures regarding their performance subject to seismic forces is one of the main research areas in structural engineering. This goal can be achieved by using structural optimization techniques [46,47]. During the optimization process, it is essential to adhere to the strength and serviceability constraints specified in contemporary earthquake codes for reinforced concrete structures. Irregularities in architectural designs, irregular geometry features, and mistakes caused by aesthetic concerns can cause serious damage or collapse of the building against seismic loads [48,49]. The response and behavior of this building structure when subjected to static and dynamic loading mostly depend on the dimensions of the sections and the spatial configuration of the columns and shear walls [50]. Although some of these irregularities can be mitigated by adjusting the cross-sectional dimensions of the structural elements, it is not always cost-effective or possible to eliminate all irregularities. Therefore, optimization emphasizes the importance of designing a structurally suitable solution that also takes into account the cost of the project [51,52].

The torsional irregularities play a crucial role in identifying structural weaknesses due to torsional forces during earthquakes. Although the significance of evaluating the seismic behavior of planar, irregularly reinforced concrete frames is highlighted, there are few investigations on the optimization of torsional irregularities in RC buildings. Goldberg [53] was one of the pioneering researchers in engineering optimization problem-solving. Following Goldberg's work, many researchers have applied various algorithms to address different structural design problems. As mentioned earlier, there are many research projects on the structural optimization of RC structures, and most of these studies focus on the cost of structures. When earthquake codes are examined, the most prominent structural irregularity is torsional irregularity. Several studies explored torsional irregularity from various aspects [54,55]. For instance, Archana and Akbar [56] focused on the torsional irregularity guidelines outlined in the Indian standard code. They analyzed 35 buildings with varying shapes related to torsional irregularity using ETABS software. They suggested recommendations aimed at refining the code to enhance the structural safety of buildings. Botis and Cerbu [57] introduced a theoretical approach to minimize torsional irregularities in multi-story concrete buildings by aligning the center of mass with the center of stiffness on each floor. They employ the MATLAB program and ETABS software for the modeling of structures. They suggested the proposed methods be examined for actual structural scenarios. Demir and Dönmez [58] investigated the torsional irregularity factors affecting multistory shear frame systems according to the Turkish Seismic Code. They considered six types of reinforced concrete buildings with different plan geometry, number of stories, and shear placements used in the study. Özmen et al. [59] investigated torsional irregularities in multistory buildings. They investigated six typical buildings with different shear locations, stories, and axis numbers. They found that the torsional irregularity increases as the number of stories decreases, with maximum irregularity coefficients occurring for single-story structures. However, due to the complexity and variability of irregular structures, there is often a lack of sufficient measured structural and ground vibration data, resulting in designs that rely on empirical or simplifying assumptions. In addition, seismic design optimization usually requires the use of optimization algorithms for searching and solving, but for irregular structures, the complexity and high dimensionality may lead to the inefficiency of traditional optimization algorithms.

In this study, the torsional irregularities of reinforced concrete structures with slab discontinuity irregularities in the plan under an earthquake were investigated and analyzed. By implementing ANN-PSO in MATLAB, the optimum dimensions of the vertical carriers were designed to bring the torsional irregularity coefficient of reinforced concrete structures to a certain limit. For this purpose, building systems, namely 3D 6-story frame systems, are modeled by the finite element method (FEM) under static and dynamic loads, and the irregularity conditions are investigated. The optimum design of the relative story drift for setting a lower limit on the torsional irregularity coefficient is realized by ANN-PSO applications. To the best of the authors' knowledge, few studies have been conducted about the application of hybrid and advanced optimization algorithms in dealing with irregular structures. On the other hand, the hybridization of PSO with ANN improves performance and yields promising results for solving complex processes and engineering problems [60,61]. In addition, in some studies, compared to the GA algorithm, PSO has fast convergence and a lower number of computational formulations [62,63]. The PSO algorithm demonstrated that it is an efficient method with the combination of ANN for modeling complex problems in various scientific fields [64,65]. The concept adopted in the present study examined the application of data-driven and meta-heuristic algorithms (i.e., ANN-PSO) in cooperation with the FEM method for the safe and economical design of RC structures.

Overall, the present study highlights the significance of eliminating torsional irregularities. This work presented a novel approach for solving torsional irregularities through coupling evolutionary algorithms and the FEM method. The findings of the research can be used by structural engineers to reduce torsional irregularities. Therefore, structural engineering can fulfill the criteria for torsional regularity and improve structural performance. In summary, the suggested approach is regarded as a reliable and efficient technique for the economic and safety design of reinforced concrete structures in seismic conditions.

2. Optimization problem

Section 2 provides a definition of an optimization problem and discusses its various components, including size optimization, objective function, design variables, and design constraints. Furthermore, it explains the mathematical definition of the optimization problem and addresses the specific issues related to irregularly reinforced concrete structures.

Optimization refers to the process of achieving the most favorable outcome given certain conditions [66]. Engineers are required to make numerous scientific and administrative decisions during every phase of the design, development, and repair of any engineering system [67–69]. The general goal of these decision-making processes is to reduce the necessary work or maximize the intended advantage.

By adjusting the member sizes of irregular structures, selecting appropriate objective functions, design variables, and constraints, and combining the search and optimization capabilities of the PSO algorithm, optimization schemes applicable to the seismic design of irregular reinforced concrete structures can be obtained. These schemes can improve the structural response to seismic forces, reduce the inter-story displacement of the structure, and give the structure better stability and safety under the action of external forces such as earthquakes. A discrete structural optimization issue is expressed by Eqs. (1) and (2).

$$\text{Objective} : \min f(\mathrm{X}), \mathrm{X} = \mathrm{X}_1, \mathrm{X}_2, \ldots, \mathrm{X}_n \tag{1}$$

$$\text{Limit} : g_j(\mathrm{X}) \leq 0, j = 1, 2, \ldots, m;\ \mathrm{X}^L \leq \mathrm{X} \leq \mathrm{X}^U \tag{2}$$

where $f(\mathrm{X})$ represents the objective function and should be minimized depending on the requirements of the problem; $g_j(\mathrm{X})$ represents inequality constraints; the number of boundaries m and the number of variables n should not be related in any way; j is an n-dimensional vector called the design variable. The variables X^L and X^U correspond to the lower and upper limits, respectively, and are called geometric or side constraints. The aforementioned mathematical model includes inequality constraints because equality constraints are typically absent in structural optimizations.

2.1. Size optimization

In size optimization problems, the cross-sectional dimensions of the structural system elements—the area or thickness of the plate—are the design variables. The connections between the different elements and the modal points of their coordinates do not change [70–72]. By using component sizes of the PSO algorithm and setting appropriate ranges and accuracies, such as upper and lower bounds, increments, etc., different combinations of component sizes can be explored during the optimization process to find a better solution.

The objective function typically encompasses the mass, stiffness, or cost of the building. Since the geometry and boundary conditions (such as loads and constraints) are already identified, these can be used to define the constraints for columns and beams with respect to geometry, strength, deformation, etc. [73–75]. The values that the design variables can take in the sizing optimization problem can be discrete or continuous. No elements of the structural system are added or removed during dimension optimization. Therefore, the size and number of elements are usually defined by designers based on their experience and structural design constraints.

2.2. Objective function

The criterion or objective function refers to the measure by which the design is optimized when represented as a function of the

design variables. For an ideal solution, the objective function should sometimes have a minimum and sometimes a maximum value [76,77]. The selection of the objective function is determined by the characteristics of the problem. In civil engineering, the objective function can be easily defined by the weight, cost, displacement, or other objectives of the building. In the seismic optimization scheme of irregular structures, a common objective function is to reduce the movement between adjacent floors. The inter-story displacement is the difference between adjacent floors and is a crucial indicator for evaluating the seismic vulnerability of structures with irregularities. By setting the objective function as the weighted sum or integrated value of the inter-story displacement and determining the weight assignment according to the importance of the structure and design requirements, the optimal design for minimizing the inter-story displacement can be achieved.

2.3. Design variables

In order to develop a mathematical formulation of the problem, some parameters of the building system must first be determined. These parameters are not changed by the optimization algorithm and are called predetermined parameters when the system is regulated. Parameters that cannot be determined a priori are called design variables. In mathematical terms, design variables can be continuous or discrete. Design variables that express the solution in structural optimization problems can take discrete values [78]. The design factors for irregularly reinforced concrete structures include the cross-sectional dimensions and the number of beams and columns. In the PSO algorithm, these design variables can be encoded in binary, integer, or real numbers and converted to actual member sizes and quantities using appropriate decoding methods. The proper selection and range setting of the design variables will have a significant impact on the optimization results.

2.4. Design constraints

Limitations related to the cross-sectional dimensions of structural elements are called design constraints. There are several constraints that need to be satisfied in order to create a design that is deemed satisfactory [79]. The minimum dimensions of a beam or the minimum thickness of a slab are important examples of design constraints. These a priori constraints arise from many different situations, such as regulatory requirements or architectural requirements. Constraints can be expressed in two different ways.

(1) Behavioral or functional constraints refer to limitations that define the boundaries of the system's behavior or performance. For instance, the behavior of maximal displacement or torsion.

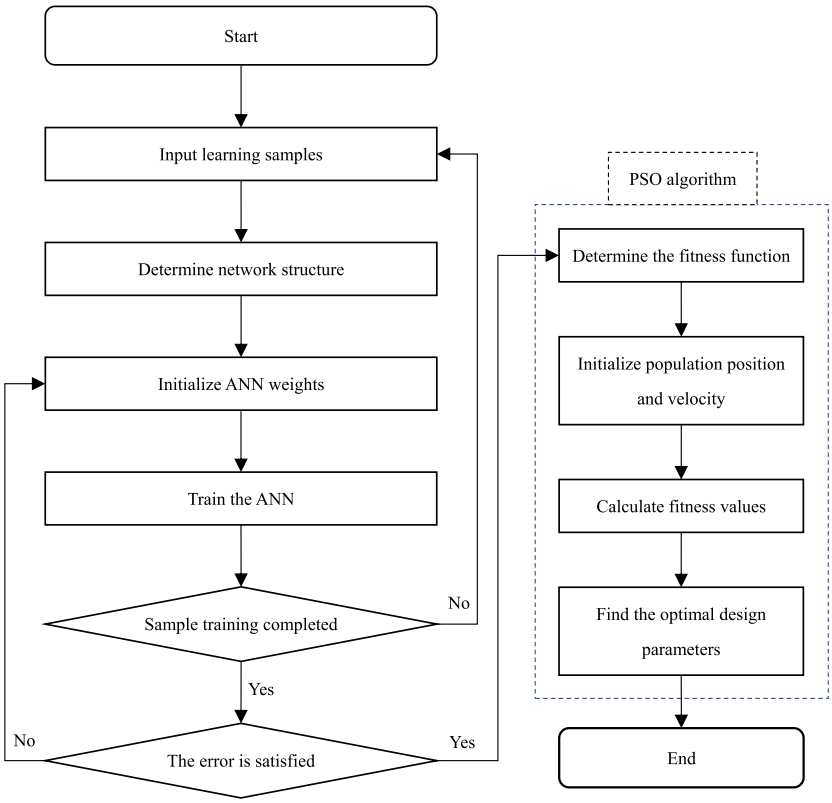

Fig. 1. ANN-PSO algorithm process.

(2) Geometric constraints refer to the restrictions that impose physical limitations on design variables, including usability and manufacturability.

During the design process, a number of variable constraints are required to be considered. For example, member dimensions need to meet the requirements of structural strength, stability, and stiffness; column spacing needs to meet the practical conditions of use and construction; member dimensions need to meet the requirements of workability and site construction, etc. These constraints can be considered by setting appropriate constraints to ensure that the optimized solution is feasible and reasonable. In the PSO algorithm, the variable restriction problem can be handled by designing a suitable fitness function or constraint function.

3. Working principle of ANN-PSO

Section 3 provides a detailed explanation of the working principle of the ANN-PSO algorithm, the specific parameters considered, and the process of optimizing the design to minimize torsional irregularities for optimal design analysis of irregular frame structures.

In this study, in view of the good performance of the ANN model in fitting problems and the good applicability of the PSO algorithm for solving engineering structure optimization problems, ANN is used as a proxy model for the PSO fitness function, and the ANN-PSO algorithm is used for optimal design analysis of irregular frame structures. ANN-PSO can exploit the nonlinear application of ANN but also overcome the ANN weights encountered at slow convergence speeds, making it easy to fall into the problem of local optimum. Its algorithm flow is shown in Fig. 1.

ANN is the most widely used intelligent algorithm based on the error backpropagation algorithm for training, which is an algorithm containing hidden layers and multilayer feedforward neural networks [80,81]. ANN inspires the action of biological neurons in the brain for the modeling and formulation of complex problems [82]. ANN can model nonlinear problems with acceptable performance [83,84]. Fig. 2 indicates the architecture of ANN. The input vector of the ANN is x, the input layer has n nodes, the hidden layer has n_1 nodes, w_i is the weight between the hidden and the output layers, θ_j is the threshold value of the output layer, and the output vector is y.

This study is based on the ANN model to fit the complex implicit relationship between the number and size of column and beam elements versus the relative inter-story drift. Different combinations of variables are selected and numerically simulated separately, and the data generated by all combinations is used as the data set for training the neural network. The data set is divided according to the ratio of 7:3. The design parameters are optimized according to the PSO-BP algorithm process. The calculation of each computational node of the ANN is as follows (Eq. (3) to (5)):

$$u_j = \sum_{i=1}^{n} w_i x_i - \theta_j \tag{3}$$

$$y_j = f(u_j) \frac{1}{1+\exp(-\lambda u_j)} \tag{4}$$

$$y_j = f'(u_j) \frac{\lambda \exp(-\lambda u_j)}{1+\exp(-\lambda u_j)} \frac{1}{1+\exp(-\lambda u_j)} = \lambda [1 - f(u_j)] f(u_j) \tag{5}$$

Output nodes of each layer can be calculated from Eqs. (6) and (7) as follows:

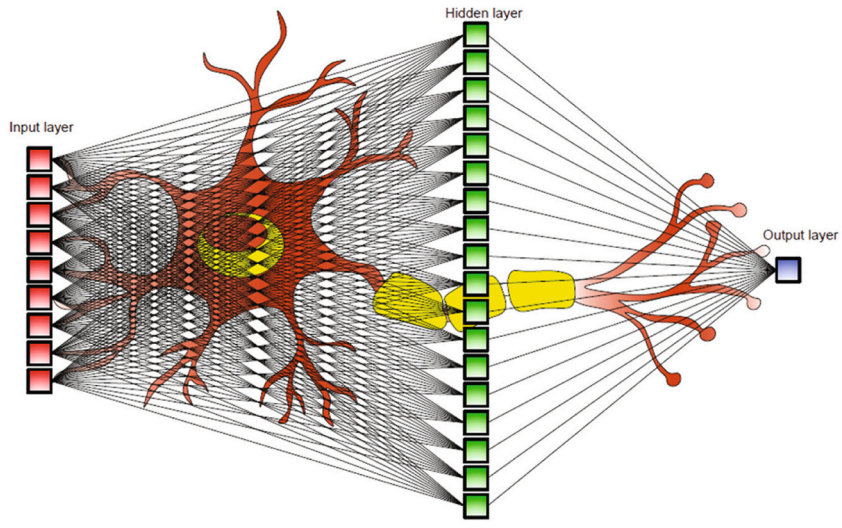

Fig. 2. The architecture of the ANN [85].

$$x_j^{'} = f\left(\sum_{i=0}^{n-1} w_{ij} - \theta_j\right), j = 0, 1, 2, \cdots, n_1 - 1 \tag{6}$$

$$y_j = f\left(\sum_{k=0}^{n_1-1} w_{ij}^{'} x^{'} - \theta_j^{'}\right), k = 0, 1, 2, \cdots, m - 1 \tag{7}$$

ANN has the ability to nonlinearly map from input to output, but it is easy to reach local minima after a certain number of iterations and other problems. Therefore, the PSO algorithm can be combined to improve it. Unlike the stochastic gradient descent method used for ANN training, the PSO algorithm is a global optimization-seeking algorithm that finds the optimal solution to the problem over the entire region. The weights and thresholds in the ANN are used as moving particles, and the positions of the particles indicate the magnitude of the current weights and thresholds. The sum of the squared deviation from the result of the neural network and the sample is used as the fitness function of the particle movement, as shown in Eq. (8).

$$J_p = \frac{1}{2}\sum_{k=1}^{N}\left[\left(y_1 - y_1^{'}\right)^2 + \left(y_2 - y_2^{'}\right)^2\right] \tag{8}$$

where y_1 is the output value of the sample, y' 1 is the resultant value of the ANN, and N is the number of groups in the number of samples. The smaller the value of J_P, the higher the fitness of the particles and the smaller the error of the neural network training. In order to calculate the optimal solution to obtain the neural network weights and thresholds, the weights and thresholds of the trained ANN are obtained by iterating Eqs. (9) and (10) according to the PSO algorithm [86].

$$V_{(n+1)} = V_{(n)}\omega + C_1 \times \mathrm{rand}(\boldsymbol{\theta}) \times \left[P_{\mathrm{best}(n)} - X_{(n)}\right] + C_2 \times \mathrm{rand}(\boldsymbol{\theta}) \times \left[G_{\mathrm{best}(n)} - X_{(n)}\right] \tag{9}$$

$$X_{n+1} = X_n + V_{n+1} \tag{10}$$

where ω is the velocity inertia number; C_1 and C_2 are learning factors; $V_{(n)}$ is the particle movement velocity; and (θ) is a random number between 0 and 1; $P_{\mathrm{best}(n)}$ is the particle position with the best adaptation during each particle movement; $G_{\mathrm{best}(n)}$ is the particle position with the best adaptation among the population particles.

4. Torsional irregularity in reinforced concrete structures

Section 4 examines torsional irregularity in reinforced concrete structures, which is a crucial concern in earthquake design. The purpose is to define torsional irregularity and establish criteria to gauge its significance. Additionally, this section presents approaches to seismic design, elaborating on static load analysis, mode combination methods, and limitations on relative floor drift. These approaches are implemented to enhance the safety and performance of structures during seismic events. It explores the mathematical and regulatory frameworks employed to evaluate and address torsional effects.

When earthquake regulations are investigated, the most prominent structural irregularity is torsional irregularity. Torsional effects create bending and additional shear forces in reinforced concrete elements. This condition is difficult to assess properly and can be destructive. If the torsional irregularity coefficient is less than 1.2, it is assumed that the torsional irregularity has no significant effect on the behavior of the structure, and no additional treatment is required.

4.1. Torsional irregularity

Torsional irregularity is deemed to be significant when the torsional irregularity coefficient η_{bi} is greater than 1.2, as shown below (Eq. (11)):

$$\eta_{\mathrm{bi}} = (\Delta_{\mathrm{i}})_{\mathrm{avg}} \Big/ (\Delta_{\mathrm{i}})_{\mathrm{max}} > 1.2 \tag{11}$$

where η_{bi} is the torsional misalignment coefficient, $(\Delta_{\mathrm{i}})_{\mathrm{avg}}$ is the average relative displacement of layer i in the same direction, and $(\Delta_{\mathrm{i}})_{\mathrm{max}}$ is the maximum relative displacement of any layer i.

4.2. Floor discontinuities

If there are large gaps in the floor slab, the rigid diaphragm behavior is impeded so that the system stiffness required by the code cannot be achieved, and then the slab in part of the floor slab is discontinuous. This includes the following three specific cases:

1) If the sum of the cavity area (including the stair cavity and elevator cavity) exceeds one-third of the total floor area, as follows (Eq. (12)):

$$\mathrm{A_b} = \mathrm{A_{b1}} + \mathrm{A_{b2}A_b/A} > 1/3 \tag{12}$$

where A_b is the sum of the void areas, and A is the gross floor area.

2) Local slab voids make safely transmitting seismic forces to vertical structural elements challenging.
3) The occurrence of sudden drops in the in-plane stiffness and strength of the slab is explained to cause slab discontinuity in the structure.

In structures where unsymmetrical slab gaps and discontinuity of beams in these areas are not provided, the largest torsional effects occur, and horizontal displacements increase. It is recommended to avoid the formation of such irregularities.

4.3. Methods used in seismic design

4.3.1. Equivalent static load analysis

In the equivalent static analysis method, the response of the structure is assumed to be linearly elastic. The total seismic force exerted on the entire structure in the considered earthquake path is determined by Eq.(13).

$$V_t = (WA(T_1) / R_a(T_1)) \geq 0.1A_0IW \tag{13}$$

where W is the whole weight of the building, A (T_1) is the spectral acceleration factor considered in determining the seismic load, A_0 is the influential ground acceleration factor, R_a (T_1) denotes the reduction factor for the seismic force, and I is the structural importance factor.

The linear distribution of this load along the height is usually preferred, so the horizontal load (Fi) acting in the direction of dynamic degrees of freedom at the first floor is equivalent and calculated according to Eq. (14).

$$F_i = (V_t - \Delta_{FN}) \frac{W_i H_i}{\sum_{j=1}^{n} W_j H_j} \tag{14}$$

$$\Delta_{FN} = 0.0075 N V_t \tag{15}$$

where w_i is the weight of the first floor of the structure, H_i is the height of the first floor of the structure measured from the top of the bottom, and Δ_{FN} is the value of the additional equivalent seismic load acting on the top floor of the structure, as determined by Eq. (15).

4.3.2. Mode combination method

In the mode combining method, other vibration periods and mode shapes are also considered to find the total earthquake load, and the related mode shapes are taken as the basis for distributing this total load to the building floors. According to Eq. (16), the ordinate of the reduced acceleration spectrum to be considered in any nth vibration mode is determined.

$$S_{ar}(T_n) = S_{ae}(T_n) g / R_a(T_n) \tag{16}$$

where S_{ar} (T_n) is the ordinate of the reduced acceleration spectrum for the nth natural vibration mode, S_{ae} (T_n) is the elastic spectral acceleration for this mode, g is the gravitational acceleration, and R_a (T_n) is the seismic load reduction coefficient for the nth natural vibration mode.

The optimal number of vibration modes Y to be included in the calculation shall be calculated based on the following rule: the total of the effective masses computed for each mode in the two vertical and horizontal seismic directions considered must always exceed 90% of the total mass of the building.

$$\sum_{n=1}^{Y} M_{xn} = \sum_{n=1}^{Y} \frac{L_{xn}^2}{M_n} \geq 0.90 \sum_{i=1}^{N} m_i \tag{17}$$

$$\sum_{n=1}^{Y} M_{mn} = \sum_{n=1}^{Y} \frac{L_{yn}^2}{M_n} \geq 0.90 \sum_{i=1}^{N} m_i \tag{18}$$

where L_{xn}, $L_{yn,}$ and modal mass M_n in Eqs. (17) and (18) are calculated by Eqs. (19)–(21), as shown below.

$$L_{xn} = \sum_{i=1}^{N} m_i \Phi_{xin} \tag{19}$$

$$L_{yn} = \sum_{i=1}^{N} m_i \Phi_{yin} \tag{20}$$

$$M_n = \sum_{i=1}^{N} \left(m_i \Phi_{xin}^2 + m_i \Phi_{yin}^2 + m_{\theta i} \Phi_{\theta in}^2 \right) \tag{21}$$

where Φ is the modal matrix, and mi is the mass of the *i*th story.

When combining mode contributions, each vibration mode calculation needs to statistically combine rules for the maximum non-simultaneous contributions of total seismic forces, internal force components, inter-story shear forces, displacements, and relative inter-story drift. These rules are: If the natural period of any two considered vibration modes always satisfies the condition $T_m/T_n < 0.80$ (where $T_m < T_n$), the square root rule (SRSS) can be applied to combine the maximum mode contributions. If this condition is not satisfied, the full quadratic combination rule will be applied to combine the maximum mode contributions. For the calculation of the cross-correlation coefficient applying this rule, the modal damping ratio of all vibration modes should be taken as 5%.

In the considered seismic direction, if the ratio of the total seismic load V_{tB} of the building found through the combined mode contribution to the total seismic load Vt of the building calculated through the equivalent seismic load method is less than the defined value β ($V_{tB} < \beta_{Vt}$), the magnitude of all internal forces and displacements found according to the combined mode method should be increased according to Eq. (22).

$$B_D = (\beta V_t / V_t B) B_B \tag{22}$$

4.3.3. Limitation of effective relative floor drift

The decreased relevant story drift, Δ_i, which represents the difference in displacement between two subsequent stories in any column (Fig. 3), shall be obtained by Eq. (23).

$$\Delta_i = d_i - d_{i-1} \tag{23}$$

where d_i and d_{i-1} show the horizontal displacements at the ends of the columns by calculating them on the *i*th and (*i* - 1)th floors of the structure.

The reduced relative inter-story drift is obtained by multiplying the relative inter-story drift by the behavior factor of the structural system. For a column at any *i*th floor of the structure in each seismic direction, the maximum value of the relative story drift $(\Delta_i)_{max}$ calculated by Eq. (23) within that floor shall satisfy one of the unfavorable conditions given in Eq. (24). According to the conditions of Eq. (25), at any floor of the structure, the rigidity of the structural system must be enhanced, and the seismic calculations shall be redone.

$$\delta_i = R\Delta_i \tag{24}$$

$$(\delta_i)_{mak} / h_i \leq 0.02 \tag{25}$$

5. Application of ANN-PSO to torsional irregularity

This section outlines the optimization problem, establishes an objective function to minimize the relative displacement between floors, and introduces the design variables and constraints according to the ACI 318–2019 Building Code. Next, it presents numerical examples illustrating the optimization of a 3D reinforced concrete building with façade irregularities. The goal of this part is to reveal the successful application of the suggested computational approach to optimizing building designs to reduce torsional irregularities and enhance seismic performance.

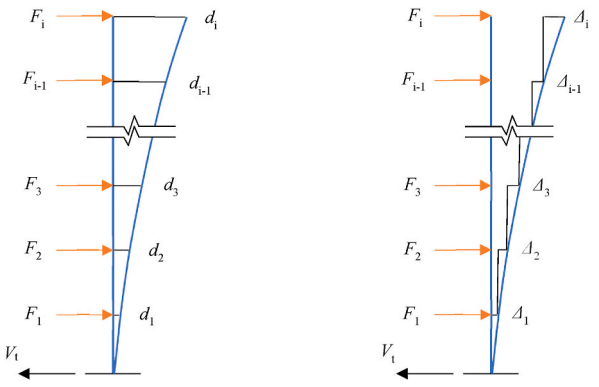

Fig. 3. Diagram of the relative displacement calculation between floors.

5.1. Objective function

Eq. (26) gives the objective function for the optimization issue of calculating the relative displacement between floors. In addition, Eqs. (27) and (28) determine the constraints of the problem.

$$\text{Objective(minimize)drift} = \left(\text{Drift(X)}^2 + \text{Drfit(Y)}^2\right)^{0.5} \tag{26}$$

$$\text{Restriction } g_j(x) \le 0 \text{ j} = 1, 2, \ldots, \text{m} \tag{27}$$

$$x^{iL} \le x \le x^{iU} \quad i = 1, 2, ..., n \tag{28}$$

where Drift(X)^2 and Drfit(Y)^2 are the relative interlayer drifts in the x and y seismic directions, respectively, the g(x) inequality and the constraint return a vector of length n. x^{iL}, x^{iu} constitute the minimum and maximum boundaries of the dimensional design variables determined by the design code.

5.2. Design variables

The variables are the number and dimensions of the columns and beam elements. The minimum and maximum quantities and dimensions are determined according to ACI 318–2019 *Building Code Requirements for Structural Concrete*. In practice, the column length is fixed, and only the thickness is a design variable.

5.3. Design constraints

Dimensional limitations: The minimum dimensions of rectangular columns permitted in ACI 318–2019 should be more than or equal to 250 × 300 mm, and the cross-sectional area should be more than or equal to 75000 mm^2. The columns' cross-sectional area should satisfy the condition that the axial compression force computed subjected to the combined N_d vertical load and seismic load should be maximum.

$$A_c \ge \sum \left(N_d / 0.5F_{ck}\right) \tag{29}$$

where N_d is the designed axial force, A_C is the entire cross-sectional concrete area in the column, and F_{ck} refers to the concrete's compressive strength.

Geometric constraints: According to Eq. (29), the columns can have a square or rectangular shape. The column's width (bc) and depth (hc) should not be smaller than the minimum dimensional limits. According to Eq. (30) and (31), the dimensions of the column are constrained to be within the following limits:

$$\left(b_{\min,i} / b_i\right) - 1 \le 0 \quad i = 1, 2, \ldots, n \tag{30}$$

$$\left(h_{\min,i} / h_i\right) - 1 \le 0 \quad i = 1, 2, \ldots, n \tag{31}$$

The variable " i " represents the index of the columns, whereas " n " represents the entire amount of columns.

Each problem should have distinct definitions for the minimal width (b_{min}) and height (h_{min}) based on the design constraints.

Compatibility constraint: The compatibility constraint ensures that the width of the column (b_c) at a given floor is not less than the width of the corresponding beam (b_w) and that the reinforcement of the beam continues along the column. During an earthquake in a building, seismic forces are generated in the junction zone, where the masses are gathered. For this reason, the column-beam joint area is an important location where its strength becomes critical. In the normalized form, this constraint can be written in the normalized form of Eq. (32).

$$1 - \left(b_c / b_w\right) \le 0 \tag{32}$$

5.4. Numerical examples

In the numerical example, the optimal design of relative inter-story displacements is achieved for a three-dimensional reinforced concrete building with a floor slab having discontinuous irregularities in the plane. In ACI 318–2019, it should be avoided that the space on the floor is larger than 1/3 of the total floor area. The building model analyzed in this paper is a 3-dimensional, 6-story frame and frame beam structural system. The total floor area is $A = 17 \times 14 = 238\ \text{m}^2$. The area of space on the floor is $Ab = 10 \times 8 = 80\ \text{m}^2$. According to Eq. (33), there are floor discontinuities existing in the building structure.

$$\frac{A_b}{A} = 0.3361 > \frac{1}{3} = 0.333 \tag{33}$$

During the analysis of the building, 65 different load combinations were used in the ETABS software package to analyze the effects of static and dynamic loads. From these load combinations, torsional irregularities under certain selected loads were analyzed. For

simplicity, anchored bearings were used in all directions. The vertical structural part of each building model was presumed to remain consistent across the vertical extent of the building. Walls are not considered as load-bearing elements in the system, and the masses of the walls are considered to be collected at the nodes of the computational model. In determining these masses, a splitting process will be applied at the center of the layer so that the upper part of the layer will be added to the mass of the upper layer, and the lower part will be added to the mass of the lower layer. The slab load consists of a dead load and a 30% live load. All internal forces and displacements obtained from the mode coupling method are scaled up according to the requirements of the lower limit values of load magnitude in ACI 318–2019. The seismic analysis was performed at ±5% eccentricity in both seismic directions. In the considered models, the floor slabs were analyzed as flexible and rigid diaphragms, respectively, and the results were compared. Since the results obtained by the two methods showed significant differences, it was decided to accept the flexible diaphragm. In order to eliminate the torsional irregularities, an ANN-PSO algorithm was used for the optimal dimensioning of the relative inter-story drift. The structural information and characteristics of the building structure are listed in Table 1.

ANN-PSO is used to minimize a nonlinear function with real-number constraints. The number of independent variables is equal to the number of members, e.g., the thickness of the columns and the height of the beams. The independent variables are used as input layer nodes, and the relative displacements between layers are used as output layer nodes. The data obtained from the simulation is used to train the ANN. The ANN model is trained using the Levenberg-Marquardt (LM) algorithm, and the transfer functions of the implicit layer and the output layer are the tansig function and the purelin function, respectively, with the implicit layer set to 1 layer and its number of neurons being 11. It is mentioned that LM is the most efficient and robust training algorithm for ANN training based on findings from previous research [87–89].

After the training, the ANN model is used as the fitness function of PSO, the number of populations is set to 30, and the number of dropping points is set to 100, so that the particle flight speed and particle flight boundary are limited to laboratory factors. The frame was solved three times, and among the solutions obtained in each group, the optimal solution was used as the best design. Table 2 shows the parameter set of PSO.

5.4.1. Load combinations used in the design

The assumed dead and live loads on each floor slab are 1.56 kN/m^2 and 2 kN/m^2, respectively. According to ACU, the following load combinations (Eq. (34) to (36)) are used when using the ETABS procedure in the design:

$$F_d = 1.4G + 1.6Q \tag{34}$$

$$F_d = G + Q \pm E \tag{35}$$

$$F_d = 0.9G \pm E \tag{36}$$

where G, Q, and E represent the dead load, the live load, and the horizontal load, respectively.

5.4.2. Prepared computer program

The ETABS structural analysis software was used to perform static and dynamic analysis of 3D reinforced concrete structures and to investigate irregularities. The application of the ANN-PSO algorithm was used for optimal sizing by connecting MATLAB and ETABS programs through an application programming interface (API). The computer used to optimize the structural dimensions has standard specifications (ASUS i5-8250U CPU, 1.80 GHz, 8 GB RAM, 64-bit SSD, Windows 10), and the computation time for one instance is about 1.5 h.

5.4.3. Example of calculation

Since the columns in the plan layout are the same for all floors, there is only one-floor group, and the variables are divided into 24 column groups. There are a total of 48 variables in each column group. In this program, there are 144 variables for the columns, for a total of 288 design variables. The upper and lower bounds for the length and width of the columns are set to 300 mm and 600 mm, respectively. In this model, all the cross-sectional dimensions of the beams are calculated in 300 mm × 500 mm dimensions, and all the columns are calculated in 500 × 500 mm pre-defined dimensions. A typical plan view of the model used for the optimization procedure

Table 1
Features and parameters of the selected building structure.

Indicators	Value	Indicators	Value
Floor height	3.0 m	Wall unit weight	4.2 kN/m^2
Laying thickness	15 cm	Seismic rating	Grade 1
Concrete grade	C25	Floor level	Z2
Concrete density	2500 kg/m^3	Spectral characteristic period	$T_A = 0.15$; $T_B = 0.40$
Modulus of elasticity	$E = 30$ GPa	Effective ground acceleration	$A_0 = 0.4$
Type of reinforcement	S420	Building importance factor	$I = 1.0$
Yield strength of reinforcement	$f_y = 420$ MPa	Damping rate	5%
Tensile strength of reinforcing bar	$f_{su} = 500$ MPa	Ductility class	High
Moving load	$q = 2$ kN/m^2	Moving Load Factor	$n = 0.3$
Wall	Full brick wall		

Table 2
The setting parameter of PSO.

Parameter	Value
Number of particles in the swarm	30
Individual learning factor	1.5
Social learning factor	1.7
Maximum number of iterations/times	100
Initial weights	0.9
Final weights	0.5
Variation probability constant	3
Optimization range of the regularization parameter	2^{-8}~2^{8}
Optimization range of the kernel function parameter	2^{-8}~2^{8}

and a 3D view of the frame model are given in Fig. 4.

It is clear from Fig. 5 that after inputting the initial data, the optimal solution was obtained by 4000 function evaluations after 20 iterations defined as a criterion for ending and with approximately the amount of time the CPU takes to complete a task 30 h. When Table 3 is analyzed, it can be seen that the torsional inequality rule coefficient in the optimal solution is very close to the limiting value. In Table 4, the sizes of the columns are shown as length and width, in accordance with the x and y axes, respectively. As a result of the ANN-PSO algorithm solution (Table 4), the dimensions and orientation of the optimized columns differ somewhat from the pre-optimized solution. Table 3 shows that in the optimized solution, the torsional irregularity coefficient in the y-direction does not exceed the limit value, and therefore, no torsional irregularity is generated.

6. Discussions

This section analyzes and interprets the results and examines the impact of dimensional optimization on a structure by comparing torsional irregularity coefficients before and after optimization. In addition, it discusses the advantages and potential limitations of the research in addressing the challenges of irregularly reinforced concrete structures.

The torsional irregularity coefficients of all floors in the structure were compared before and after the application of dimensional optimization, and the results obtained are summarized in Fig. 6; the "optimal solution" and the "initial solution" of the models are compared in the Y-direction. It can be seen that, as a result of the dimensional optimization, the torsional irregularity of each floor of the model does not exceed the limits specified by ACI 318–2019. In addition, the torsional irregularity coefficients in both directions do not exceed the limit values in the optimized solution for each floor and do not cause torsional irregularities.

The proposed approach eventually leads to economic design optimization of seismic-RC 3D buildings. The advantages of this approach include its robustness and effectiveness in its ability to determine the best solution for the economical and safe design of RC structures. Furthermore, the proposed approach illustrates the use of MATLAB and ETABS through an application programming interface (API), highlighting the integration capabilities with software tools. In the following, an overview of the advantages and limitations of the introduced method is discussed. The proposed method offers several advantages. This study provided a systematic and efficient technique for finding the best design solution, considering constraints related to torsional irregularity, and leading to optimized RC frames that meet the requirements of torsional irregularity coefficients. The use of the ANN-PSO algorithm implemented in the MATLAB program and the finite element method conducted in ETABS software generated an efficient optimization method for

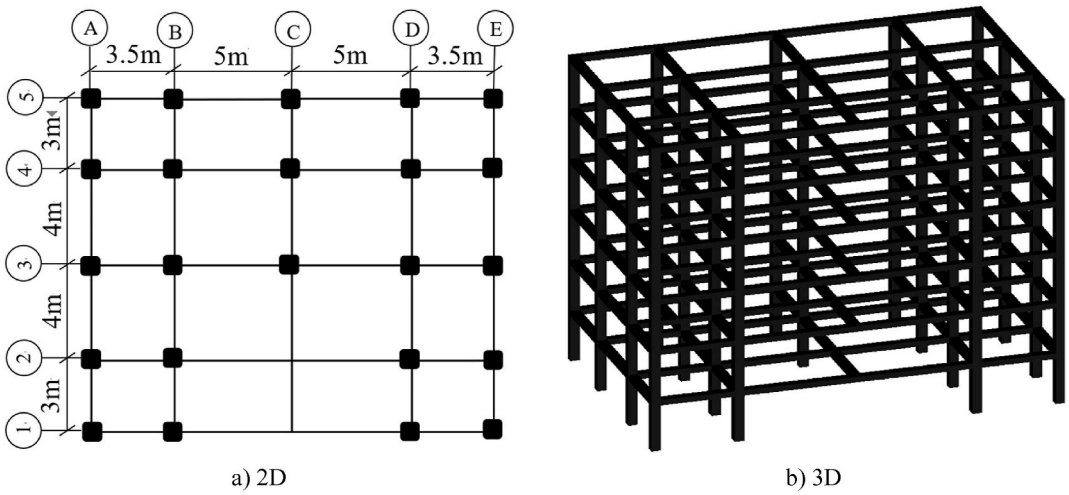

Fig. 4. View of the frame model, a) 2D and b) 3D.

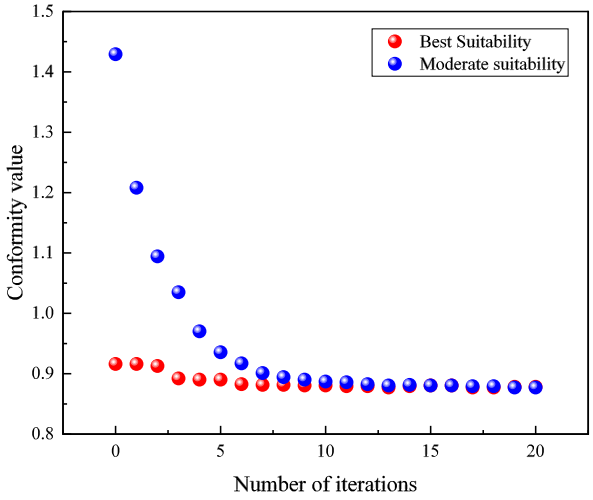

Fig. 5. ANN-PSO algorithm convergence trend.

Table 3
Initial and optimal torsion coefficients.

Number of floors	X - earthquake direction		Y - earthquake direction	
	Initial coefficients	Optimal torsion coefficients	Initial coefficients	Optimal torsion coefficients
1	1.08	1.03	1.30	1.20
2	1.09	1.04	1.17	1.09
3	1.09	1.05	1.13	1.08
4	1.10	1.05	1.11	1.09
5	1.11	1.05	1.10	1.08
6	1.11	1.06	1.12	1.13

Table 4
The initial and optimal column sizes.

Column number	b_c		h_c	
	Initial size (mm)	Optimal Size (mm)	Initial size (mm)	Optimal Size (mm)
1	500	557	500	346
2	500	472	500	387
3	500	514	500	409
4	500	563	500	401
5	500	594	500	312
6	500	502	500	382
7	500	462	500	409
8	500	549	500	345
9	500	589	500	402
10	500	573	500	415
11	500	562	500	360
12	500	591	500	350
13	500	451	500	400
14	500	494	500	394
15	500	528	500	345
16	500	592	500	340
17	500	591	500	410
18	500	575	500	360
19	500	523	500	354
20	500	457	500	400
21	500	591	500	315
22	500	594	500	305
23	500	509	500	390
24	500	498	500	350

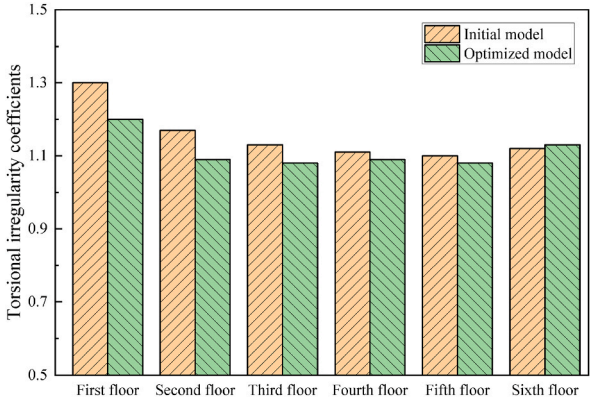

Fig. 6. Comparing the initial and best solutions of torsional irregularity coefficients.

economic design optimization of seismic reinforced concrete 3D structures.

Stability analysis involves the evaluation of the structural response and behavior, which includes reducing inter-story displacement, preventing torsional irregularities, and enhancing the seismic performance of the structures. Stability analysis is crucial to ensuring that the optimized design solutions satisfy the criteria of structural stability, safety, and performance under seismic loading conditions. It involves the assessment of various factors such as inter-story drift, torsional irregularity coefficients, and the overall structural response to external forces, specifically seismic forces. The proposed method aims to improve the seismic performance of the structures, reduce inter-story displacement, and enhance stability and safety under external forces such as earthquakes.

The present study suggests an innovative method that involves modeling the RC frames using the finite element method and subjecting them to static and dynamic loads. Subsequently, the cross-sections of columns are optimized to restrict the torsional irregularity coefficient of the structures to a certain limit. The study also considered the limitations and constraints associated with the design process, such as the minimum dimensions of columns allowed based on the ACI 318–2019 Building Code Requirements for structural concrete. Nevertheless, the potential limitations of optimization problems related to the convergence speed of the evolutionary algorithm can be influenced by the complexity and large-scale RC structures. In large-scale structures, the optimization algorithm may need more iterations to converge on an optimal solution. Moreover, fine-tuning of the internal parameters of PSO may be necessary to achieve optimal results.

7. Conclusions

The conclusion section summarizes the key findings of the study and their implications. In addition, this section provides recommendations for future studies or practical applications based on the research outcomes. Torsion behavior is critical to consider in irregular RC structures, as excessive torsional effects might result in structural failure. Torsional irregularity coefficients play a crucial role in reducing torsional damage caused by earthquakes and ensuring the safety of structures. It effectively addressed torsional irregularities in reinforced concrete buildings. The purpose of this study is to investigate the torsional irregularities of irregular three-dimensional frame-reinforced concrete structures under static and dynamic loads and to eliminate the torsional irregularities by using the ANN-PSO algorithm implemented in the MATLAB program and the finite element method conducted via ETABS software for optimizing the RC structure. The availability of the ANN-PSO algorithm and MATLAB for optimal sizing of structures is demonstrated by connecting MATLAB and ETABS through an application programming interface (API). The ANN-PSO algorithm type is a robust and effective tool suitable for solving civil engineering problems, and the best solution for economic design optimization of seismic reinforced concrete 3D structures is determined using this algorithm.

The results indicated that the ANN-PSO technique efficiently optimizes the dimensions of columns and achieves values of the torsional irregularity coefficients that are very close to the minimum. The study's insights into the optimization problem, size optimization, and numerical examples make significant contributions to the ongoing efforts to enhance the structural performance of structures under seismic forces. The findings demonstrated that the approach was highly efficient in optimizing the dimensions of columns to match the criteria for torsional inequality coefficients, thereby preventing any occurrence of torsional irregularities. The study also highlighted the use of the ANN-PSO algorithm for optimal design analysis of irregular frame structures. The results showed that the torsional irregularity coefficients did not exceed the limit values in the optimized solution, effectively eliminating torsional irregularities. The cross-sectional dimensions of columns play a crucial role in determining the structural behavior and load-carrying capacity of the RC frames. Optimizing these dimensions can lead to more efficient and cost-effective designs. The design constraints ensure that the dimensions of the columns in the irregular RC structures meet the necessary requirements for structural stability, safety, and process to ensure practical and feasible solutions.

The present study proposes a novel method to improve the performance, efficiency, and safety of structural RC by facilitating the systematic exploration and optimization of design variables. This method allows designers to consider a wide range of design options to find the most efficient and effective solutions within the constraints of stability and safety criteria. The suggested method can be

employed to address complex design problems and find solutions that may not be easily achievable through manual design procedures, thereby leading to time and resource savings and cost-effectiveness in the design and Construction of RC frames. This method can improve the seismic performance of RC structures by optimizing design variables, such as the cross-sectional area of columns, while considering design constraints.

For future studies, the suggested method in the present study can consider multiple objective functions for solving irregularity torsion. In addition, it may be necessary to evaluate the findings of the research through further investigations and testing to ensure the effectiveness and practicality of the proposed method in real-world applications. Moreover, it is interesting that the suggested method is conducted on different types of frames, such as steel or timber frames. It is worth mentioning that although the earlier studies and results obtained indicated the efficiency and robustness of the PSO algorithm for solving complex problems, it is useful to conduct comparative studies between the proposed method and other evolutionary algorithms to assess the performance and effectiveness of the ANN-PSO method for optimization of RC frames.

In summary, the findings of the study have significant implications for the development of more efficient and reliable design and optimization approaches in structural engineering. This has the potential to enhance the safety and resilience of RC structures. Moreover, the successful application of the suggested method for seismic design optimization of irregular RC buildings highlights the importance of advanced computational approaches in improving structural stability and safety against external forces such as earthquakes.

Data availability statement

All data generated or analyzed during this study are included in this published article.

CRediT authorship contribution statement

Xun Zhang: Investigation.

Declaration of competing interest

The authors declare that they have no known competing financial interests or personal relationships that could have appeared to influence the work reported in this paper.

References

[1] Z. Wang, Q. Wang, C. Jia, J. Bai, Thermal evolution of chemical structure and mechanism of oil sands bitumen, Energy (Oxford) 244 (2022) 1, https://doi.org/10.1016/j.energy.2022.123190, 10.1016/j.energy.2022.123190.
[2] W. Liu, J. Liang, T. Xu, Tunnelling-induced ground deformation subjected to the behavior of tail grouting materials, Tunn. Undergr. Space Technol. 140 (2023) 105253, https://doi.org/10.1016/j.tust.2023.105253.
[3] H. He, J. Shi, S. Yu, J. Yang, K. Xu, C. He, X. Li, Exploring green and efficient zero-dimensional carbon-based inhibitors for carbon steel: from performance to mechanism, Construct. Build. Mater. 411 (2024) 134334, https://doi.org/10.1016/j.conbuildmat.2023.134334.
[4] Z. Shu, B. Ning, J. Chen, Z. Li, M. He, J. Luo, H. Dong, Reinforced moment-resisting glulam bolted connection with coupled long steel rod with screwheads for modern timber frame structures, Earthq. Eng. Struct. Dynam. 52 (4) (2023) 845–864, https://doi.org/10.1002/eqe.3789.
[5] H. Ding, L.Q. Chen, Shock isolation of an orthogonal six-DOFs platform with high-static-low- dynamic stiffness, J. Appl. Mech. 90 (2023) 111004, https://doi.org/10.1115/1.4062886.
[6] C. Ren, J. Yu, X. Liu, Z. Zhang, Y. Cai, Cyclic constitutive equations of rock with coupled damage induced by compaction and cracking, Int. J. Min. Sci. Technol. 32 (5) (2022) 1153–1165, https://doi.org/10.1016/j.ijmst.2022.06.010.
[7] C. Ren, J. Yu, C. Zhang, X. Liu, Y. Zhu, W. Yao, Micro–macro approach of anisotropic damage: a semi-analytical constitutive model of porous cracked rock, Eng. Fract. Mech. 290 (2023) 109483, https://doi.org/10.1016/j.engfracmech.2023.109483.
[8] H. Huang, M. Guo, W. Zhang, M. Huang, Seismic behavior of strengthened RC columns under combined loadings, J. Bridge Eng. 27 (6) (2022) 05022005, https://doi.org/10.1061/(ASCE)BE.19435592.0001871.
[9] L. Yang, M. Ye, Y. Huang, J. Dong, Study on mechanical properties of displacement-Amplified Mild steel bar joint damper, Iranian Journal of Science and Technology, Transactions of Civil Engineering (2023) 1–14, https://doi.org/10.1007/s40996-023-01268-7.
[10] H. Huang, M. Li, W. Zhang, Y. Yuan, Seismic behavior of a friction-type artificial plastic hinge for the precast beam-column connection, Arch. Civ. Mech. Eng. 22 (4) (2022) 201, https://doi.org/10.1007/s43452-022-00526-1.
[11] J. Zhang, C. Zhang, Using viscoelastic materials to mitigate earthquake-induced pounding between adjacent frames with unequal height considering soil-structure interactions, Soil Dynam. Earthq. Eng. 172 (2023) 107988, https://doi.org/10.1016/j.soildyn.2023.107988.
[12] S.T.R.O.I.A.N.O.V.S.K.Y.I. Dmytro, The study of welding requirements during construction and installation of seismic-resistant steel structures, Journal of Research in Science, Engineering and Technology 8 (2) (2020) 17–20, https://doi.org/10.24200/jrset.vol8iss2pp17-20.
[13] X. Zhang, G. Zhou, X. Liu, Y. Fan, E. Meng, J. Yang, Y. Huang, Experimental and numerical analysis of seismic behaviour for recycled aggregate concrete filled circular steel tube frames, Comput. Concr. 31 (6) (2023) 537–543, https://doi.org/10.12989/cac.2023.31.6.537.
[14] B. Pang, H. Zheng, Z. Jin, D. Hou, Y. Zhang, X. Song, M. Li, Inner superhydrophobic materials based on waste fly ash: Microstructural morphology of microetching effects, Compos. B Eng. 268 (2024) 111089, https://doi.org/10.1016/j.compositesb.2023.111089.
[15] H. Huang, Y. Yuan, W. Zhang, M. Li, Seismic behavior of a replaceable artificial controllable plastic hinge for precast concrete beam-column joint, Eng. Struct. 245 (2021) 112848, https://doi.org/10.1016/j.engstruct.2021.112848.
[16] J.X. Lin, G. Chen, H.S. Pan, Y.C. Wang, Y.C. Guo, Z.X. Jiang, Analysis of stress-strain behavior in engineered geopolymer composites reinforced with hybrid PE-PP fibers: a focus on cracking characteristics, Compos. Struct. 323 (2023) 117437, https://doi.org/10.1016/j.compstruct.2023.117437.
[17] C. Zhou, J. Wang, X. Shao, L. Li, J. Sun, X. Wang, The feasibility of using ultra-high performance concrete (UHPC) to strengthen RC beams in torsion, J. Mater. Res. Technol. 24 (2023) 9961–9983, https://doi.org/10.1016/j.jmrt.2023.05.185.
[18] Y. Yao, L. Zhou, H. Huang, Z. Chen, Y. Ye, Cyclic performance of novel composite beam- to-column connections with reduced beam section fuse elements, in: Structures, vol. 50, Elsevier, 2023, April, pp. 842–858, https://doi.org/10.1016/j.istruc.2023.02.054.
[19] X. Zhang, X. Liu, S. Zhang, J. Wang, L. Fu, J. Yang, Y. Huang, Analysis on displacement-based seismic design method of recycled aggregate concrete-filled square steel tube frame structures, Struct. Concr. (2023), https://doi.org/10.3390/ma16124268.

[20] X. Zhang, S. Wang, H. Liu, J. Cui, C. Liu, X. Meng, Assessing the impact of inertial load on the buckling behavior of piles with large slenderness ratios in liquefiable deposits, Soil Dynam. Earthq. Eng. 176 (2024) 108322, https://doi.org/10.1016/j.soildyn.2023.108322.
[21] J. Li, Y. Liu, G. Lin, Implementation of a coupled FEM-SBFEM for soil-structure interaction analysis of large-scale 3D base-isolated nuclear structures, Comput. Geotech. 162 (2023) 105669, https://doi.org/10.1016/j.compgeo.2023.105669.
[22] X. Shi, Y. Yang, X. Zhu, Z. Huang, Stochastic dynamics analysis of the rocket shell coupling system with circular plate fasteners based on spectro-geometric method, Compos. Struct. 329 (2024) 117727, https://doi.org/10.1016/j.compstruct.2023.117727.
[23] F. Aslanova, A comparative study of the hardness and force analysis methods used in truss optimization with metaheuristic algorithms and under dynamic loading, Journal of Research in Science, Engineering and Technology 8 (1) (2020) 25–33, https://doi.org/10.24200/jrset.vol8iss1pp25-33.
[24] D. Li, J.H. Nie, H. Wang, W.X. Ren, Loading condition monitoring of high-strength bolt connections based on physics-guided deep learning of acoustic emission data, Mech. Syst. Signal Process. 206 (2024) 110908, https://doi.org/10.1016/j.ymssp.2023.110908.
[25] M. Wang, X. Yang, W. Wang, Establishing a 3D aggregates database from X-ray CT scans of bulk concrete, Construct. Build. Mater. 315 (2022) 125740, https://doi.org/10.1016/j.conbuildmat.2021.125740.
[26] J. Cao, H. He, Y. Zhang, W. Zhao, Z. Yan, H. Zhu, Crack detection in ultrahigh-performance concrete using robust principal component analysis and characteristic evaluation in the frequency domain, Struct. Health Monit. (2023) 14759217231178457, https://doi.org/10.1177/14759217231178457.
[27] Y. Tang, Y. Wang, D. Wu, M. Chen, L. Pang, J. Sun, W. Feng, X. Wang, Exploring temperature- resilient recycled aggregate concrete with waste rubber: an experimental and multi-objective optimization analysis, Rev. Adv. Mater. Sci. 62 (1) (2023) 20230347, https://doi.org/10.1515/rams-2023-0347.
[28] M. Ghasemi, M. Samadi, E. Soleimanian, K.W. Chau, A comparative study of black-box and white-box data-driven methods to predict landfill leachate permeability, Environ. Monit. Assess. 195 (7) (2023) 862, https://doi.org/10.1007/s10661-023-11462-9.
[29] M. Torabi, H. Sarkardeh, S.M. Mirhosseini, Prediction of soil permeability coefficient using the GEP approach, Numerical Methods in Civil Engineering 7 (1) (2022) 9–15.
[30] M. Samadi, H. Sarkardeh, E. Jabbari, Prediction of the dynamic pressure distribution in hydraulic structures using soft computing methods, Soft Comput. 25 (2021) 3873–3888, https://doi.org/10.1007/s00500-020-05413-6.
[31] R. Kazemi, H. Eskandari-Naddaf, T. Korouzhdeh, New insight into the prediction of strength properties of cementitious mortar containing nano-and micro-silica based on porosity using hybrid artificial intelligence techniques, Struct. Concr. (2023), https://doi.org/10.1002/suco.202200101.
[32] Y. Peng, C. Unluer, Modeling the mechanical properties of recycled aggregate concrete using hybrid machine learning algorithms, Resour. Conserv. Recycl. 190 (2023) 106812, https://doi.org/10.1016/j.resconrec.2022.106812.
[33] R.S. Suri, V. Dubey, N.R. Kapoor, A. Kumar, M. Bhushan, Optimizing the compressive strength of concrete with altered compositions using hybrid PSO-ANN, in: International Conference on Information Systems and Management Science, Springer International Publishing, Cham, 2021, December, pp. 163–173, https://doi.org/10.1007/978-3-031-13150-9_15.
[34] A.N. Hanoon, A.W. Al Zand, Z.M. Yaseen, Designing new hybrid artificial intelligence model for CFST beam flexural performance prediction, Eng. Comput. 38 (4) (2022) 3109–3135, https://doi.org/10.1007/s00366-021-01325-7.
[35] M. Ahmadi, M. Kioumarsi, Predicting the elastic modulus of normal and high strength concretes using hybrid ANN-PSO, Mater. Today: Proc. (2023), https://doi.org/10.1016/j.matpr.2023.03.178.
[36] H. Mashhadban, S.S. Kutanaei, M.A. Sayarinejad, Prediction and modeling of mechanical properties in fiber reinforced self-compacting concrete using particle swarm optimization algorithm and artificial neural network, Construct. Build. Mater. 119 (2016) 277–287, https://doi.org/10.1016/j.conbuildmat.2016.05.034.
[37] M.A. Bayari, N. Shabakhty, E. Izadi Zaman Abadi, Estimating collapse risk and reliability of concrete moment frame structure using response surface method and hybrid of artificial neural network with particle swarm optimization algorithm, in: Proceedings of the Institution of Mechanical Engineers, Part O: Journal of Risk and Reliability, vol. 235, 2021, pp. 1072–1089, https://doi.org/10.1177/1748006X211007424, 6.
[38] T.H. Nguyen, N.L. Tran, V.T. Phan, D.D. Nguyen, Prediction of shear capacity of RC beams strengthened with FRCM composite using hybrid ANN-PSO model, Case Stud. Constr. Mater. (2023) e02183, https://doi.org/10.1016/j.cscm.2023.e02183.
[39] M. Afzal, Y. Liu, J.C. Cheng, V.J. Gan, Reinforced concrete structural design optimization: a critical review, J. Clean. Prod. 260 (2020) 120623, https://doi.org/10.1016/j.jclepro.2020.120623.
[40] G. Sánchez-Olivares, A. Tomás, Improvements in meta-heuristic algorithms for minimum cost design of reinforced concrete rectangular sections under compression and biaxial bending, Eng. Struct. 130 (2017) 162–179, https://doi.org/10.1016/j.engstruct.2016.10.010.
[41] W.K. Hong, M.C. Nguyen, T.D. Pham, Pre-tensioned concrete beams optimized with a unified unction of objective (UFO) using ANN-based Hong-Lagrange method, J. Asian Architect. Build Eng. (2023) 1–23, https://doi.org/10.1080/13467581.2023.2270028.
[42] H. Yazdani, M. Khatibinia, S. Gharehbaghi, K. Hatami, Probabilistic performance-based optimum seismic design of RC structures considering soil-structure interaction effects, ASCE-ASME Journal of Risk and Uncertainty in Engineering Systems, Part A: Civil Engineering 3 (2) (2017) G4016004, https://doi.org/10.1061/AJRUA6.0000880.
[43] M.J. Esfandiari, G.S. Urgessa, S. Sheikholarefin, S.D. Manshadi, Optimum design of 3D reinforced concrete frames using DMPSO algorithm, Adv. Eng. Software 115 (2018) 149–160, https://doi.org/10.1016/j.advengsoft.2017.09.007.
[44] A.M. Martins, L.M. Simões, J.H. Negrão, A.V. Lopes, Sensitivity analysis and optimum design of reinforced concrete frames according to Eurocode 2, Eng. Optim. 52 (12) (2020) 2011–2032, https://doi.org/10.1080/0305215X.2019.1693554.
[45] P.E. Mergos, Surrogate-based optimum design of 3D reinforced concrete building frames to Eurocodes, Developments in the Built Environment 11 (2022) 100079, https://doi.org/10.1016/j.dibe.2022.100079.
[46] Z. Sadat, A.S. Arslan, Genetic Algorithm approach in the prevention of torsional irregularity in reinforced concrete structures, Journal of the Faculty of Engineering and Architecture of Gazi University 37 (3) (2022) 1469–1482, https://doi.org/10.17341/gazimmfd.971104.
[47] S. Tesfamariam, M. Sanchez-Silva, A model for earthquake risk management based on the life-cycle performance of structures, Civ. Eng. Environ. Syst. 28 (3) (2011) 261–278, https://doi.org/10.1080/10286608.2011.588329.
[48] S.C. Dutta, S. Kumar, P.S. Bhoyar, M.A. Hussain, Sajal, Behavior of vertically irregular structures near mines: Comparison of responses under seismic and mine blast-induced ground motion, Struct. Des. Tall Special Build. 31 (1) (2022) e1897, https://doi.org/10.1002/tal.1897.
[49] R. Suhendra, Z. Djauhari, R. Suryanita, E. Yuniarto, Effect of flat slab to progressive collapse on irregular structures building, in: E3S Web of Conferences, vol. 156, EDP Sciences, 2020 05002, https://doi.org/10.1051/e3sconf/202015605002.
[50] H. Chaulagain, H. Rodrigues, J. Jara, E. Spacone, H. Varum, Seismic response of current RC buildings in Nepal: a comparative analysis of different design/construction, Eng. Struct. 49 (2013) 284–294, https://doi.org/10.1016/j.engstruct.2012.10.036.
[51] T. Ajay, N. Parthasarathi, M. Prakash, K.S. Satyanarayanan, Effect of planar irregularity of linear static and dynamic analysis, Mater. Today: Proc. 40 (2021) S56–S63, https://doi.org/10.1016/j.matpr.2020.03.499.
[52] E. Meral, Determination of seismic isolation effects on irregular RC buildings using friction pendulums, in: Structures, vol. 34, Elsevier, 2021, December, pp. 3436–3452, https://doi.org/10.1016/j.istruc.2021.09.062.
[53] D.E. Goldberg, Optimization Machine Learning, Addison-Wesley, Boston, MA, USA, 1989.
[54] L. He, Y. Wang, Y. Liu, X. Yu, Y. Bai, Seismic collapse performance of reinforced concrete moment frame structures with plan irregularity, Struct. Des. Tall Special Build. 31 (5) (2022) e1916, https://doi.org/10.1002/tal.1916.
[55] S.C. Alih, M. Vafaei, Performance of reinforced concrete buildings and wooden structures during the 2015 Mw 6.0 Sabah earthquake in Malaysia, Eng. Fail. Anal. 102 (2019) 351–368, https://doi.org/10.1016/j.engfailanal.2019.04.056.
[56] A.R. Archana, M.A. Akbar, A critical review of displacement-based criteria for torsional irregularity of buildings, J. Inst. Eng.: Series A 102 (4) (2021) 1169–1175, https://doi.org/10.1007/s40030-021-00579-0.
[57] M.F. Botis, C. Cerbu, A method for reducing of the overall torsion for reinforced concrete multi- storey irregular structures, Appl. Sci. 10 (16) (2020) 5555, https://doi.org/10.3390/app10165555.

[58] A. Demir, D. Donmez, Çok KATLI YAPILARDA BURULMA DÜZENSİZLİĞİNE ETKİ EDEN FAKTÖRLER, Celal Bayar University Journal of Science 4 (1) (2008) 31–36.

[59] G. Özmen, K. Girgin, Y. Durgun, Torsional irregularity in multi-story structures, International Journal of Advanced Structural Engineering (IJASE) 6 (2014) 121–131, https://doi.org/10.1007/s40091-014-0070-5.

[60] E. Viera-Martin, J.F. Gómez-Aguilar, J.E. Solís-Pérez, J.A. Hernández-Pérez, R.F. Escobar-Jiménez, Artificial neural networks: a practical review of applications involving fractional calculus, The European Physical Journal Special Topics 231 (10) (2022) 2059–2095, https://doi.org/10.1140/epjs/s11734-022-00455-3.

[61] T. Liu, Z. Ren, C. Xiong, W. Peng, J. Wu, S. Huang, G. Liang, B. Sun, Optoacoustic classification of diabetes mellitus with the synthetic impacts via optimized neural networks, Heliyon 9 (10) (2023) e20796, https://doi.org/10.1016/j.heliyon.2023.e20796.

[62] J.E. Solís-Pérez, J.F. Gómez-Aguilar, J.A. Hernández, R.F. Escobar-Jiménez, E. Viera-Martin, R.A. Conde-Gutiérrez, U. Cruz-Jacobo, Global optimization algorithms applied to solve a multi-variable inverse artificial neural network to improve the performance of an absorption heat transformer with energy recycling, Appl. Soft Comput. 85 (2019) 105801, https://doi.org/10.1016/j.asoc.2019.105801.

[63] F. Didi, M.S. Chaouche, M. Amari, A. Guezmir, K. Belhenniche, A. Chellali, Design and simulation of grid-connected photovoltaic system's performance analysis with optimal control of maximum power point tracking MPPT based on artificial intelligence, Tobacco Regulatory Science (TRS) (2023) 1074–1098.

[64] A. Coronel-Escamilla, F. Torres, J.F. Gómez-Aguilar, R.F. Escobar-Jiménez, G.V. Guerrero-Ramírez, On the trajectory tracking control for an SCARA robot manipulator in a fractional model driven by induction motors with PSO tuning, Multibody Syst. Dyn. 43 (2018) 257–277, https://doi.org/10.1007/s11044-017-9586-3.

[65] M. Umar, Z. Sabir, M.A.Z. Raja, J.G. Aguilar, F. Amin, M. Shoaib, Neuro-swarm intelligent computing paradigm for nonlinear HIV infection model with CD4+ T-cells, Math. Comput. Simulat. 188 (2021) 241–253, https://doi.org/10.1016/j.matcom.2021.04.008.

[66] M.A. Shayanfar, M.A. Barkhordari, M. Ghanooni-Bagha, Estimation of corrosion occurrence in RC structure using reliability based PSO optimization, Period. Polytech. Civ. Eng. 59 (4) (2015) 531–542, https://doi.org/10.3311/PPci.7588.

[67] J. Zhu, B. Zhou, Optimization design of RC ribbed floor system using eagle strategy with particle swarm optimization, Comput. Mater. Continua (CMC) 62 (1) (2020), https://doi.org/10.32604/cmc.2020.06655.

[68] X.L. Chen, J.P. Fu, J.L. Yao, J.F. Gan, Prediction of shear strength for squat RC walls using a hybrid ANN-PSO model, Eng. Comput. 34 (2018) 367–383, https://doi.org/10.1007/s00366-017-0547-5.

[69] A. Kaveh, R.A. Izadifard, L. Mottaghi, Optimal design of planar RC frames considering CO2 emissions using ECBO, EVPS and PSO metaheuristic algorithms, J. Build. Eng. 28 (2020) 101014, https://doi.org/10.1016/j.jobe.2019.101014.

[70] G. Zhang, B. Sun, W. Bai, H. Zhang, Prediction of the yield performance and failure mode of RC columns under cyclic-load by PSO-BP neural network, Buildings 12 (5) (2022) 507, https://doi.org/10.3390/buildings12050507.

[71] B. Wang, W. Gong, Y. Wang, Z. Li, H. Liu, Prediction of the yield strength of RC columns using a PSO-LSSVM model, Appl. Sci. 12 (21) (2022) 10911, https://doi.org/10.3390/app122110911.

[72] J. Huang, M. Zhou, J. Zhang, J. Ren, N.I. Vatin, M.M.S. Sabri, The use of GA and PSO in evaluating the shear strength of steel fiber reinforced concrete beams, KSCE J. Civ. Eng. 26 (9) (2022) 3918–3931, https://doi.org/10.1007/s12205-022-0961-0.

[73] S. Chutani, J. Singh, Use of modified hybrid PSOGSA for optimum design of RC frame, J. Chin. Inst. Eng. 41 (4) (2018) 342–352, https://doi.org/10.1080/02533839.2018.1473804.

[74] A. Kartci, A. Agambayev, M. Farhat, N. Herencsar, L. Brancik, H. Bagci, K.N. Salama, Synthesis and optimization of fractional-order elements using a genetic algorithm, IEEE Access 7 (2019) 80233–80246, https://doi.org/10.1109/ACCESS.2019.2923166.

[75] M. Babaei, M. Mollayi, Multi-objective optimal design of reinforced concrete frames using two meta-heuristic algorithms, Journal of Engineering Research 9 (4B) (2021).

[76] G. Minafò, G. Camarda, An open-source GA framework for optimizing the seismic upgrading design of RC frames through BRBs, Eng. Struct. 251 (2022) 113508, https://doi.org/10.1016/j.engstruct.2021.113508.

[77] M. Mangal, M. Li, V.J. Gan, J.C. Cheng, Automated clash-free optimization of steel reinforcement in RC frame structures using building information modeling and two-stage genetic algorithm, Autom. ConStruct. 126 (2021) 103676, https://doi.org/10.1016/j.autcon.2021.103676.

[78] M.H. Gao, X. Xie, T. Huang, N. Zhang, Y. Wang, Glutaraldehyde-assisted crosslinking in regenerated cellulose films toward high dielectric and mechanical properties, Cellulose 29 (15) (2022) 8177–8194, https://doi.org/10.1007/s10570-022-04785-2.

[79] A. Katkhoda, Optimization in the selection of structural systems for the design of reinforced concrete high-rise buildings in resisting seismic forces, Energy Proc. 19 (2012) 269–275, https://doi.org/10.1016/j.egypro.2012.05.206.

[80] J.E. Solís-Pérez, J.A. Hernández, A. Parrales, J.F. Gómez-Aguilar, A. Huicochea, Artificial neural networks with conformable transfer function for improving the performance in thermal and environmental processes, Neural Network. 152 (2022) 44–56, https://doi.org/10.1016/j.neunet.2022.04.016.

[81] M. Samadi, E. Jabbari, H.M. Azamathulla, M. Mojallal, Estimation of scour depth below free overfall spillways using multivariate adaptive regression splines and artificial neural networks, Engineering Applications of Computational Fluid Mechanics 9 (1) (2015) 291–300, https://doi.org/10.1080/19942060.2015.1011826.

[82] M. Cervantes-Bobadilla, J. García-Morales, R.F. Escobar-Jiménez, J.A. Hernández-Pérez, J.F. Gómez-Aguilar, V.H. Olivares-Peregrino, Experimental implementation of a new control approach using an inverse neural network to on-demand hydrogen production, Control Eng. Pract. 105 (2020) 104631, https://doi.org/10.1016/j.conengprac.2020.104631.

[83] D.A. Carbot-Rojas, R.F. Escobar-Jiménez, J.F. Gómez-Aguilar, J. García-Morales, A.C. Téllez-Anguiano, Modelling and control of the spark timing of an internal combustion engine based on an ANN, Combust. Theor. Model. 24 (3) (2020) 510–529, https://doi.org/10.1080/13647830.2019.1704888.

[84] M. Samadi, M.H. Afshar, E. Jabbari, H. Sarkardeh, Prediction of current-induced scour depth around pile groups using MARS, CART, and ANN approaches, Mar. Georesour. Geotechnol. 39 (5) (2021) 577–588, https://doi.org/10.1080/1064119X.2020.1731025.

[85] S. Malazdrewicz, Ł. Sadowski, An intelligent model for the prediction of the depth of the wear of cementitious composite modified with high-calcium fly ash, Compos. Struct. 259 (2021) 113234, https://doi.org/10.1016/j.compstruct.2020.113234.

[86] Ö. Günal, M. Akpinar, Solving the laminar boundary layer problem in heat transfer with heuristic optimization techniques, Heliyon 9 (6) (2023) e16955, https://doi.org/10.1016/j.heliyon.2023.e16955.

[87] A. Parrales, J.A. Hernández-Pérez, O. Flores, H. Hernandez, J.F. Gómez-Aguilar, R. Escobar-Jiménez, A. Huicochea, Heat transfer coefficients analysis in a helical double-pipe evaporator: Nusselt number correlations through artificial neural networks, Entropy 21 (7) (2019) 689, https://doi.org/10.3390/e21070689.

[88] A. Namigtle-Jiménez, R.F. Escobar-Jiménez, J.F. Gómez-Aguilar, C.D. García-Beltrán, A.C. Téllez-Anguiano, Online ANN-based fault diagnosis implementation using an FPGA: application in the EFI system of a vehicle, ISA Trans. 100 (2020) 358–372, https://doi.org/10.1016/j.isatra.2019.11.003.

[89] H.B. Ly, M.H. Nguyen, B.T. Pham, Metaheuristic optimization of Levenberg-Marquardt-based artificial neural network using particle swarm optimization for prediction of foamed concrete compressive strength, Neural Comput. Appl. 33 (24) (2021) 17331–17351, https://doi.org/10.1007/s00521-021-06321-y.